Anbar Journal of Engineering Science (AJES) **Vol. 14 , No. 1 (2023) , pp. 7 ~ 14**
P-ISSN: 1997-9428 ; E-ISSN: 2705-7440 DOI: http://doi.org/10.37649/aengs.2023.137844.1036

University of Anbar

Anbar Journal of Engineering Science©

journal homepage: https://ajes.uoanbar.edu.iq/

Thermal Analysis of Switched Reluctance Motor Based on RMXprt/Motor-CAD

Hussein Ali Bardan[a], Amer Mejbel Ali[b]
[a, b] *Electrical Engineering Department, College of Engineering, Mustansiriyah University, Baghdad, Iraq*

PAPER INFO

Paper history
Received: 02/12/2022
Revised: 14/01/2023
Accepted: 15/02/2023

Keywords:
thermal, LPTN, steady state, SRM, Motor-CAD, RMXprt.

ABSTRACT

Switched reluctance motor (SRM) is an electric motor works based on the reluctance torque produced due to the variation of the rotor pole position concerning stator poles. This paper adopts a thermal analysis on a 4-phase, 8/6 pole, 550W, SRM. Lumped parameters thermal network method(LPTN) is used in this analysis based on a combination of RMXprt/Motor-CAD software, in two-dimensional (2D), steady-state, with different cooling methods, and with different loading conditions. Motor losses like core losses, copper losses, and mechanical losses are regarded as the heat sources in SRM, which are calculated by RMXprt software. The thermal analysis achieved by Motor-CAD includes displaying the temperature distribution on different motor parts like stator winding, stator poles, stator yoke, rotor poles, rotor yoke, shaft, covers, and housing. The analysis showed the increasing temperature distribution on different motor parts with increasing motor loading conditions. Also, this temperature distribution is recorded using three different cooling methods. The comprehensive thermal analysis applied in this work will assist the motor designer in choosing a better motor thermal design without needing to produce and test costly prototype motors.

1. Introduction

SRM is a type of electric motor whose work depends on the variation of stator winding inductance, which changes according to the position of the rotor poles to the stator poles. SRM acquires attention in industrial applications such as dehumidifiers, water well pumps, vacuum cleaners, winders, blowers, fans, hoists, and conveyors [1]. SRM has advantages like winding in the stator only, simple cooling, small inertia, and robustness [2]. SRM runs at high power, so the coil and motor housing's temperature may increase significantly, making it challenging to industrialize some applications that need dynamic performance to be high [3]. In recent years, several methodologies have been introduced to study the thermal analysis of the SRM. Yukum analyzed 12/8 SRM, by using workbench software (2D FEA), the transient analysis method to determine temperature distribution in the motor, and the external circuit is utilized to supply total motor losses while using the orthogonal decomposition method to analyze iron losses and assumed that the proposed method is feasible and correct. Also, this method can be used in other types of motors [4]. Krzysztof analyzed SRM based on FEA to determine torque and Motor-CAD to determine the temperature for different combinations of stator/rotor poles 8/6, 10/8, and

* Corresponding author: Hussein Ali Bardan; *eema2015@uomustansiriyah.edu.iq* ; 0 7833494583

6/4 [5]. Jer analyzed 12/8 SRM, 3kW using computational fluid dynamics (CFD) to determine the motor's temperature distribution and JMAG-Designer software to determine iron losses [6]. Han analyzed 18/12 SRM, 30kW, by using Solidworks to build the model of SRM. Also Ansys fluent and JMAG are used to determine temperature distribution and electromagnetic torque, respectively, and the obtained results showed that cooling by water enhanced SRM temperature [7]. Hau analyzed 8/6 SRM using flux2D software to determine temperature distribution and iron losses [8]. Michael analyzed 24/16 SRM, 60kW by using Motor-CAD Ansys to determine temperature distribution based on lumped parameter thermal network (LPTN) with different speed values to estimate temperature rise in different machine components [9]. Pedram analyzed four-phase 8/6 SRM by using FEA to determine motor losses, and also used CFD Ansys to build 3D thermal model in order to forecast the temperature on the housing of the SRM, taking into account the surface temperature distribution as a signature for fault prediction an SRM's heat transmission [10]. Hung analyzed 12/8 SRM, 110kW using Maxwell Ansys to determine motor losses and workbench Ansys to determine motor temperature distribution in the rotor and stator winding [11]. Esmail analyzed 75kW, three-phase 72/48 SRM using CFD software based on 3D FEA to determine temperature distribution in the motor parts using the cooling method by a water jacket. The results clarified the existence of higher temperatures in the motor winding [12]. Emmanuel analyzed three-phase 4kW 12/8 SRM using Maxwell2D software to determine flux, torque, core losses, and copper losses, and adopted workbench software to determine temperature distribution in the rotor, stator, winding, housing with using the water jacket cooling method [13]. Renata analyzed three-phase 2kW, 6/4SRM using Maxwell2D software to determine motor torque, current, and flux linkage and adopted workbench software to determine the internal temperature rise, which is maximum in winding [14]. Pavan analyzed three-phase 6/4 SRM using CFD software to determine heat distribution in the stator, and rotor in a 3D FEM steady-state analysis [15]. Vijayakumar analyzed three-phase 6/4 SRM by using FEA to determine torque, inductance, and temperature using soft magnetic composite (SMC). He concluded that SMC was used as the magnetic core of the SRM enhanced its temperature distribution [16]. Using the liquid cooling method, Nasim analyzed 10kW, 12/8 double stator SRM by using 3D FEA to determine temperature distribution in various parts of the SRM [17]. This paper aims to perform a thermal analysis on 8/6, 550W SRM based on the combination of RMXprt/Motor-CAD software, with studying the effect of changing motor cooling methods (with and without fins and fan) and changing the loading conditions on the temperature distribution inside the motor. The main contribution of this paper is by using data taken from RMXprt software to build SRM thermal model by Motor-CAD.

2. Mathematical model of SRM

Figure1. Clarified losses distribution in SRM, which are considered as heat sources inside it.

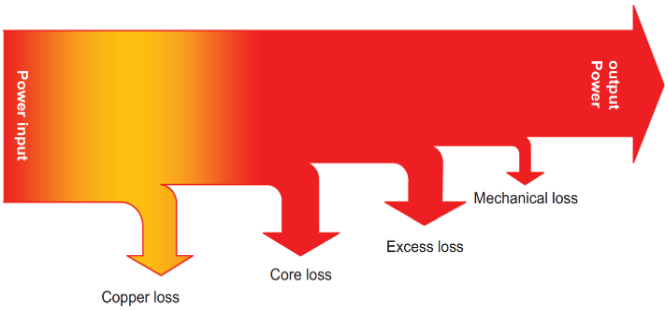

Figure1. Distribution losses in SRM.

Heat rise in SRM due to the generated power loss by various physical mechanisms which are classified into different types such as iron(core), mechanical (friction and windage), copper, and excess losses.

The equation for determining copper losses (P_{cu})is given:

$$P_{cu} = q\, I^2\, R$$
$$= q\, I^2 \rho \frac{l}{s} \quad (1)$$

Where q is the number of phases, I is RMS phase current, R is stator resistance per phase, ρ is the conductor resistivity, $\boldsymbol{\ell}$ is conductor length, and s is the conductor cross-sectional area.

The equation for determining the conductor resistivity (ρ) with temperature changes is given:

$$\rho = \rho_0\, [1 + \alpha(T - T_0)] \quad (2)$$

Where T_0 is the initial temperature in Kelvin, T is the final temperature, α is the temperature coefficient of resistivity, and ρ_0 is initial resistivity.

The equation for computing the core loss (P_{core}) is given:

$$P_{core} = P_h + P_e + P_{ex} \quad (3)$$

Where P_h, P_e, and P_{ex} represent hysteresis loss, eddy current loss, and excess loss, respectively.

The equation for friction and windage loss(P_{fw}) for the small SRM machine, such as studied in this paper, is given by:

$$P_{fw} = 2\ D^3\ Ln^3 \times 10^{-6} + G_n\ K_{fb} \times 10^{-3} \quad (4)$$

Where D denotes the outer rotor diameter in meters, n motor speed in rpm, L is stack length in meters, and K_{fb} frictional loss coefficient, G_n weight of the rotor in kg [1].

The equation for determining the SRM total losses (P_T) is given [18].:

$$P_T = P_{cu} + P_{core} + P_{fw} \quad (5)$$

The equation for determining heat flux density(q) which follows Fourier's law density, is given by:

$$q = -\lambda \frac{d_T}{dx} \quad (6)$$

Where T is the substance temperature in Kelvin, the negative sign refers to the direction in which temperature flows to a location with low temperature, and λ is the material's thermal conductivity in (W/ (m K)).

For the cooling equation, the heat flux(q) is given by:

$$q = h(T - T_f) \quad (7)$$

Where h is convective and the coefficient of the heat transfer in (W/m^2k), T_f is the temperature of the fluid medium on the boundary surface, and T denotes the temperature of the object in Kelvin.

The equation for determining the generation heat in the rotor and stator core (Q) is given:

$$Q = \frac{P_{core}}{V} \quad (8)$$

Where V denotes the corresponding part volume in m^3[19].

3. Modelling and simulation of SRM

RMXprt is a bundle of interactive software for designing and analyzing electrical machines. The electrical machine design tool uses templates and offers quick, accurate results for machine performance analysis via analysis [20]. Motor-CAD is a software available commercially for thermal analysis that uses a 3D lumped model parameter circuit, it can model electric machines in transient and steady-state thermal conditions [1]. RMXprt is used to build the SRM thermal model in Motor-CAD by exporting the RMXprt full model into Motor-CAD. The SRM model used in this study contains 4 stator phases, 8 poles in the stator and 6 poles in the rotor as illustrated in the figure2, with a rated voltage of 240V DC, speed of 1500rpm, rated power of 550W, and the steel material used is M19-24G, wire diameter equals 0.5733 mm which calculated by RMXprt based on the motor design dimensions listed in table 1 which were taken from [21] and motor data listed in table 2.

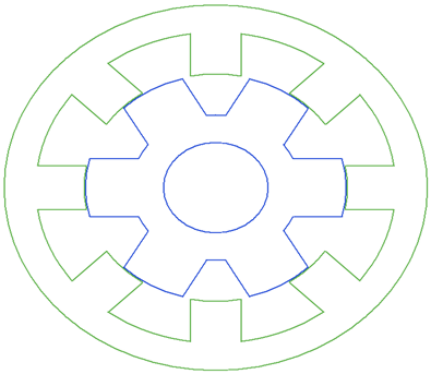

Figure2.SRM model by RMXprt.

Table1. SRM design dimensions.

Parameter	Value
Outside stator diameter	120mm
Inside stator diameter	75mm
Outside rotor diameter	74mm
Inside rotor diameter	30mm
Stator yoke thickness	9mm
Rotor yoke thickness	9mm
Stack length	65mm
Stacking factor	0.95

Table.2 SRM data.

Number of strands	1
Parallel branch	1
Wire insulation thickness	0.08mm
Number of turns per pole	142
Insulation thickness	0.3mm
Diode drop	2 V
Transistor drop	2 V
Frictional loss	12W

The radial view of SRM by Motor-CAD is clarified in figure3.

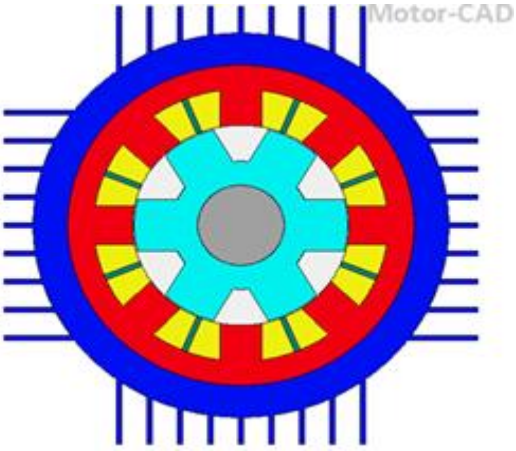

Figure.3 Radial view of SRM by Motor-CAD.

The axial view SRM by Motor-CAD is illustrated in figure4.

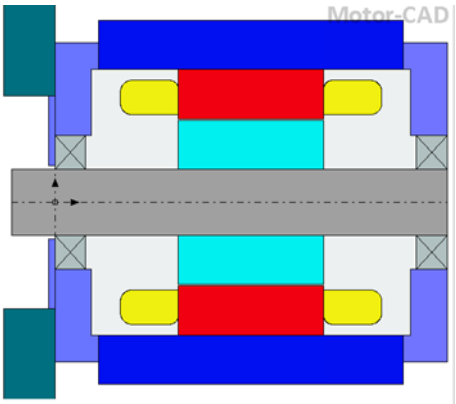

Figure4. Axial view of SRM by Motor-CAD.

Table.3 clarified different losses in SRM which are taken from RMXprt and used as input data to Motor-CAD.

Table.3 SRM losses taken from RMXprt

Component	P [Input]	Speed [REF]	Coef [A]	W/kg	P [speed]
Units	Watts	rpm		W/kg	Watts
Loss [Armature Copper]	176.6	1404	0	285.2	176.6
Loss [Stator Back Iron]	16.34	1404	1.5	10.59	16.34
Loss [Stator Tooth]	8.169	1404	1.5	10.46	8.169
Loss [Rotor Back Iron]	16.34	1404	1.5	30.13	16.34
Loss [Rotor Tooth]	8.169	1404	1.5	10.92	8.169
Loss[Friction -F Bearing]	6	1404	1	0	6
Loss [Friction-R Bearing]	6	1404	1	0	6
Loss [Windage]	0	1404	3	0	0
Loss [Windage] (Ext Fan)	0	1404	3	0	0

In Motor-CAD, the thermal network for SRM is illustrated in figure 5, lumped parameter thermal network (LPTN) is one of the most method important utilized in the thermal analysis of electrical machines because it gives the most details about temperature calculating and how heat is transferred, and also renders a quick method for scanting temperature distribution within electric machines, and allows the user to quickly calculate the changes brought on by changing input parameters. LPTN models contain different components like thermal capacitance and thermal

resistance, being lumped into simplified areas that represent complex geometry like stator teeth, rotor teeth, and poles number. LPTN cognates the electrical circuit where current denotes heat flow, voltage denotes temperature, capacitance, and resistance denotes thermal capacitance and thermal resistance. Each node in the network represents a specific scanted position in the motor's geometry, which is connected to other nodes utilizing a computed thermal resistance [1]. In a steady-state analysis of SRM, the thermal circuit comprises thermal resistance and thermal sources linked between component nodes of the motor.

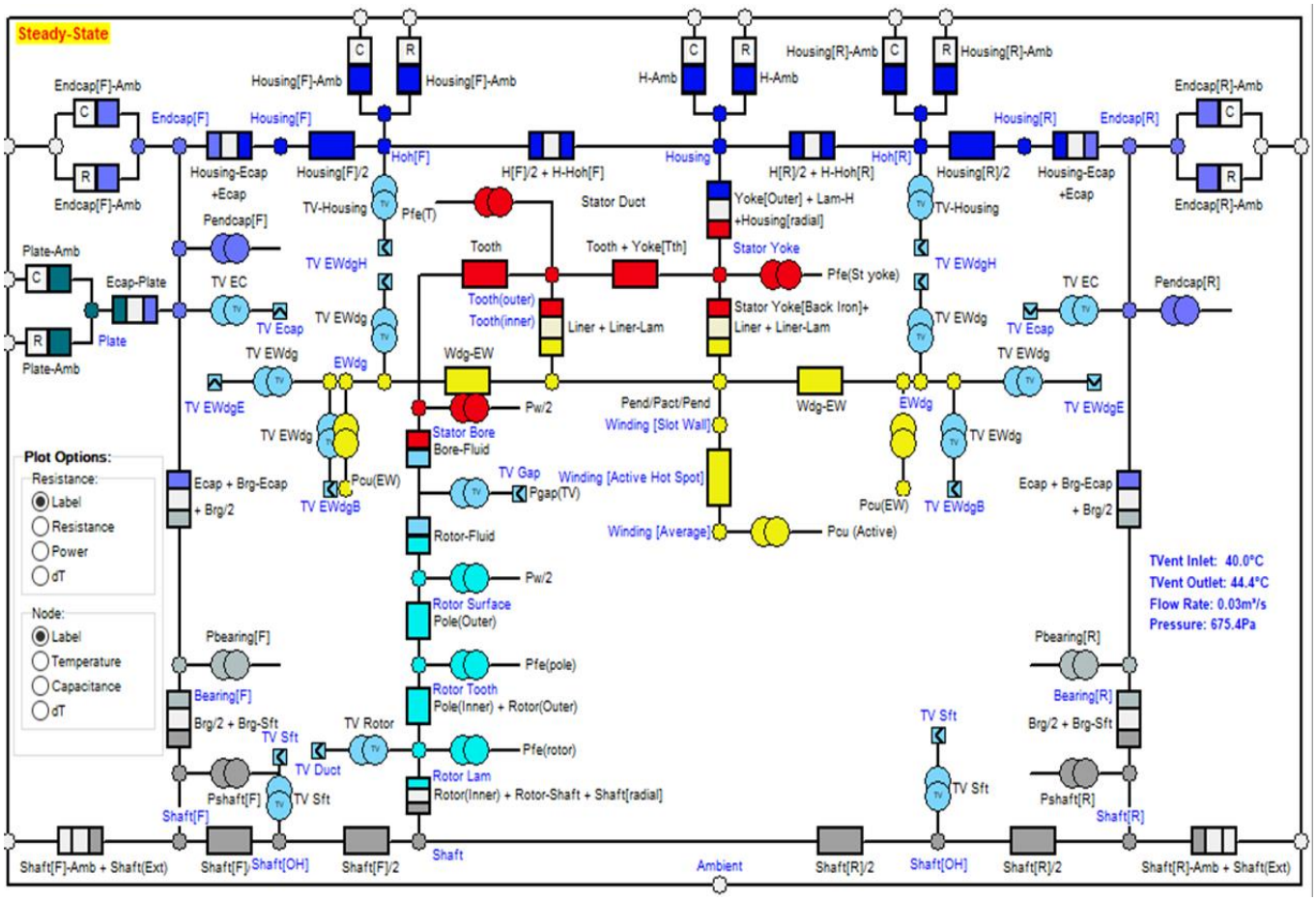

Figure 5. LPTN of SRM by Motor-CAD.

4. Results and Discussion

Figure 6 clarified temperature distribution in each part of the radial view of SRM in a steady state at full load condition with fins on the motor housing and using the cooling fan. The minimum value for temperature in housing equals 73.7°C while the maximum value for temperature distributed in winding where the maximum value for winding temperature is 166°C, the average temperature is 118.1°C and the minimum temperature is 79.4°C.

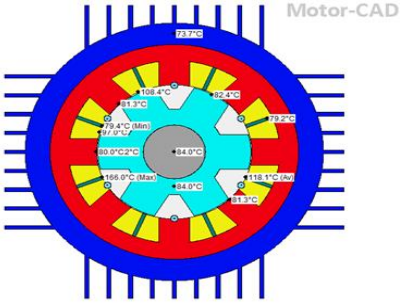

Figure6. Radial SRM model by Motor-CAD.

Figure 7 illustrates temperature distribution in the axial view of SRM in each component in the same condition mentioned above. The minimum temperature is 47.3°C in the front-end rotor cover and the maximum temperature is 166°C in the rear-end winding of the stator because it is considered the major source of heat in SRM.

Figure.8 explains the comparison between the distributed temperature in the stator winding (maximum winding temperature, average winding temperature, minimum winding temperature), housing, rotor pole, rotor yoke, shaft, and stator yoke in the three cases, case 1: motor housing without fins, and also without a fan, case 2: motor housing with fins and without the fan, case 3: motor housing with fins and with the fan. The steady-state analysis shows case 3 has the lowest temperature distribution inside the SRM.

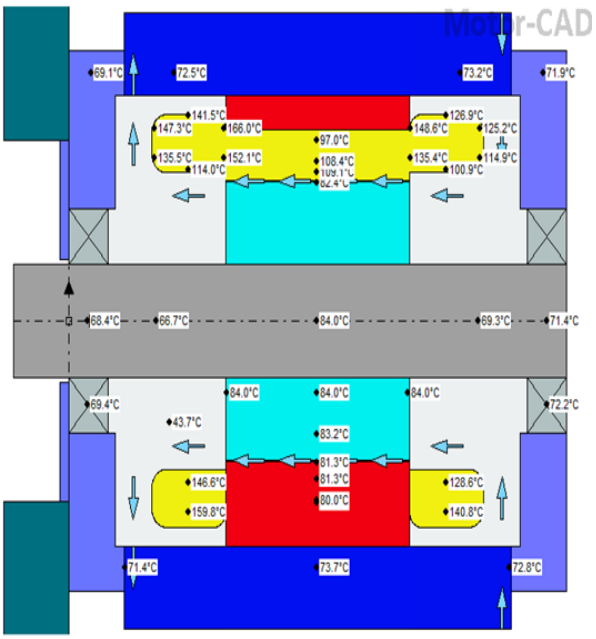

Figure7. Axial SRM model by Motor-CAD.

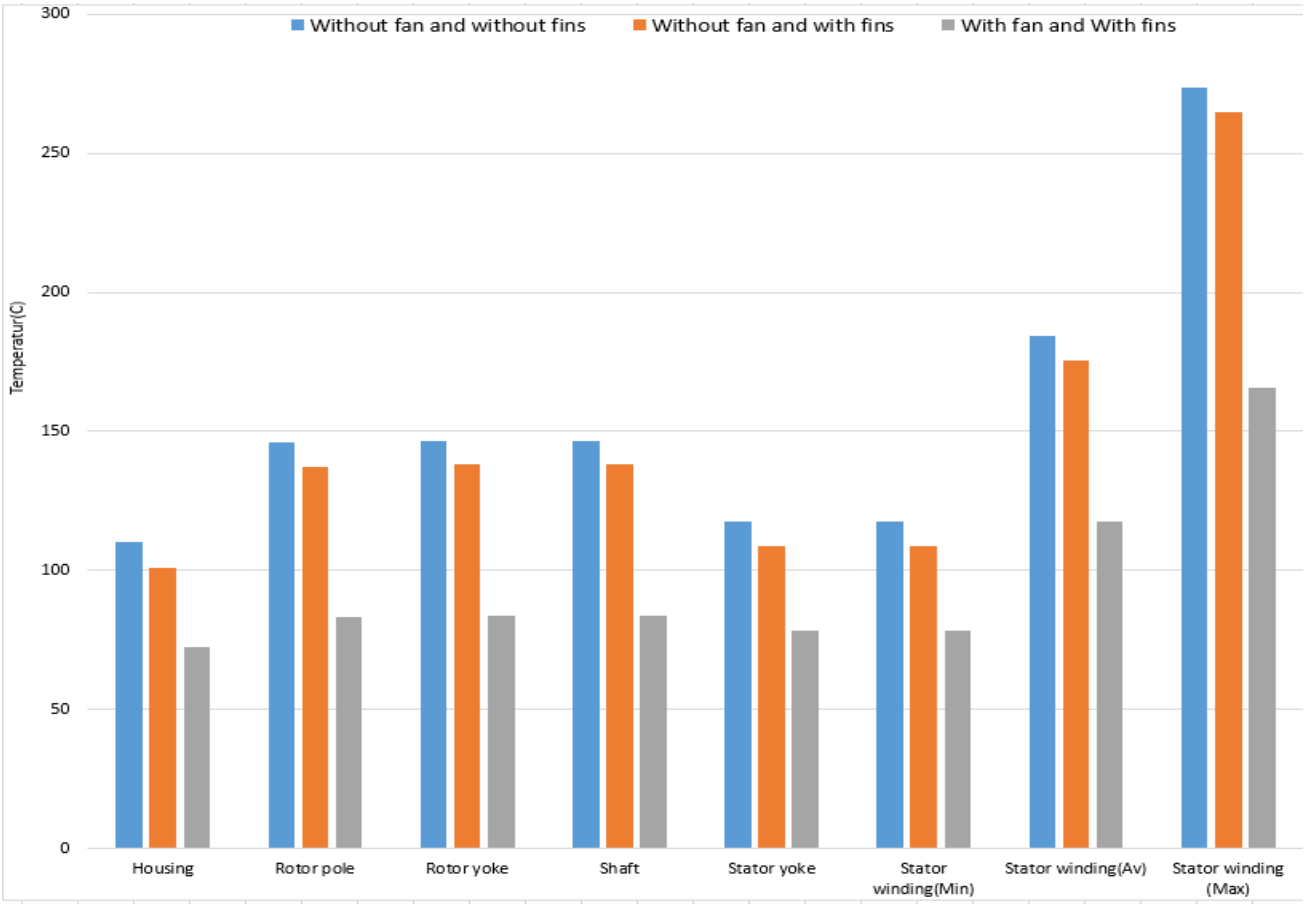

Figure 8. Temperature distribution in SRM with and without fins and fan.

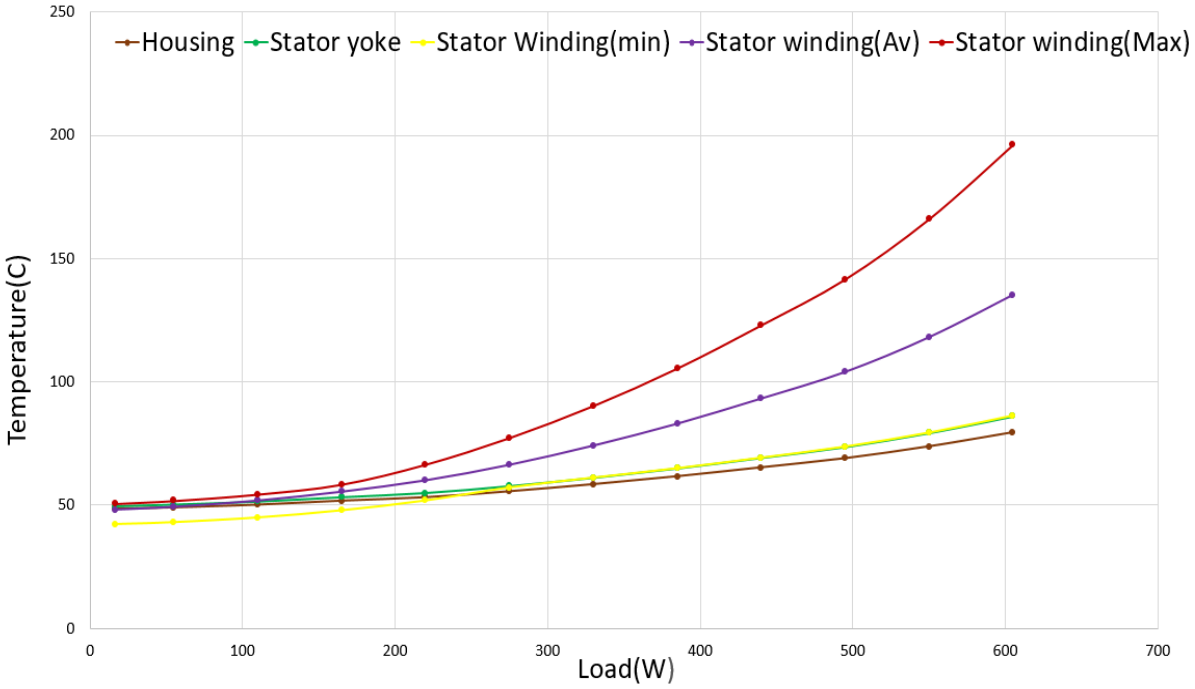

Figure 9. The temperature of the SRM parts with different loading conditions.

Figure 9 explains the varying temperature of the SRM parts with different loading conditions with fins and with the fan (from no load to 1.1% of full load) in a steady state, which showed that when the load increased, the temperature increased gradually. The maximum temperature appeared in the winding due to a higher amount of copper losses generated in it. When the motor load is low, there is an increase in the motor speed, and the SRM has minimum copper and iron losses. Therefore, the temperature of motor parts is low, as shown in figure.9, and this temperature gradually increases with an increase in load.

5. Conclusion

The thermal analysis of SRM was successfully adopted based on a combination of RMXprt/Motor-CAD software. The obtained results showed the increase of motor parts temperature with increasing the motor loading. Also, these results showed the importance of selecting a proper cooling method (using housing fins and cooling fan) to minimize the motor temperature, which will give a good guide for the motor designer to improve the SRM thermal design without needing to produce and test costly prototype motors.

Acknowledgements

Praise God, that the research has been completed after a time of investigation and patience with the problems we encountered in the study. I would want to express my appreciation and gratitude to the Electrical Engineering Department, College of Engineering, Mustansiriyah University

References

[1] B. Biligin, J. W. Jiang, and A. Emadi, "Switched reluctance motor drives: fundamentals to applications," *Boca Raton, FL, CRC Press,* 2018.

[2] R. Krishnan, "*Switched reluctance motor drives: modeling, simulation, analysis, design, and applications," Boca Raton*, CRC Press, 2017.

[3] X. Sun, B. Wan, G. Lei, X.Tian, Y. Guo, & J. Zhu, "Multiobjective and multiphysics design optimization of a switched reluctance motor for electric vehicle applications," *IEEE Transactions on Energy Conversion.*, vol. 36, pp. 3294–3304, Dec. 2021, doi: 10.1109/TEC.2021.3078547

[4] Y.Sun, B.Zhang, Y.Yuan, and F.Yang, "Thermal characteristics of switched reluctance motor under different working conditions," *Progress In Electromagnetics Research M*, vol. 74, pp. 1123, Oct.

2018,doi:10.2528/PIERM18071301

[5] K.Bieńkowski, M. Szulborski, S.Łapczyński, Ł.Kolimas, and H.Cichecki, "Parameterized 2D Field Model of a Switched Reluctance Motor," *Electricity*, vol. 2, pp. 590–613, Dec. 2021, doi. org/10.3390/electricity2040034.

[6] J. H. Jang, H. C. C hiu, W. M. Yan, M. C. Tsai, and P. Y. Wang, "Numerical study on electromagnetics and thermal cooling of a switched reluctance motor," *Case Studies in Thermal Engineering.*, vol. 6, pp. 16–27, Sep.2015,doi.org/10.1016/j.csite.2015.05.00 1

[7] H. C. Chiu, J. H. Jang, W. M. Yan, and R. B. Shiao, "Thermal performance analysis of a 30 kW switched reluctance motor," *International Journal of Heat and Mass Transfer.*, vol. 114, pp. 145–154. Nov. 2017, doi.org/10.1016/j.ijheatmasstransfer.2017.0 6.057

[8] H. Chen, W. Yan, and C. C. Chan, "Iron loss and temperature field analysis of four-phase 8/6 structure switched reluctance motor for electric vehicles," in *2019 IEEE Vehicle Power and Propulsion Conference (VPPC)*, Oct. 2019, pp. 1–4, doi: 10.1109/VPPC46532.2019.8952232

[9] M. Kasprzak, J. W. Jiang, B. Bilgin, and A. Emadi, "Thermal analysis of a three-phase 24/16 switched reluctance machine used in HEVs," in *2016 IEEE Energy Conversion Congress and Exposition (ECCE)*, Sep. 2016, pp. 1–7, doi: 10.1109/ECCE.2016.7855510

[10] P. S. Nasab, M. Moallem, E. S. Chaharsoghi, C.Caicedo-Narvaez, and B. Fahimi,., "Predicting temperature profile on the surface of a switched reluctance motor using a fast and accurate magneto-thermal model," *IEEE Transactions on Energy Conversion.*, vol. 35, pp. 1394–1401, Sep. 2020, doi: 10.1109/TEC.2020.2974789

[11] J. L. Huang, Y.Xuan, L. Zhang, and T. G. Liu, "Analysis on the design and temperature field of switched reluctance motor for electric vehicle," in *Journal of Physics: Conference Series*, vol. 1777, p. 12001, Feb. 2021, doi 10.1088/1742-6596/1777/1/012001.

[12] E. Elhomdy, Z. Liu, and G. Li, "Thermal and mechanical analysis of a 72/48 switched reluctance motor for low-speed direct-drive mining applications," *Applied Sciences.*, vol. 9, p. 2722, Jul. 2019, doi.org/10.3390/app9132722.

[13] E. C. Abunike, O. I. Okoro, and I. E. Davidson, "Thermal Analysis of an Optimized Switched Reluctance Motor for Enhanced Performance," in *2021 IEEE PES/IAS PowerAfrica*, pp. 1–5, Aug 2021, doi: 10.1109/PowerAfrica52236.2021.9543275

[14] R. R. Reis, M. L. Kimpara, J. O. Pinto, and B. Fahimi, "Multi-physics simulation oF 6/4 switched reluctance motor by finite element method,". Eletrôn. Potên., Fortaleza , v. 26, p. 8-18 Jun 2020, doi.org/10.18618/REP.2021.1.0004.

[15] A. Pavan, N. Sathyanarayanan, R. Kumar, N. C. Lenin, and R. Sivakumar, "Thermal Investigation of a Switched Reluctance Motor," *International Journal of Electrical Engineering.*, vol. 8, no. 2, pp. 115–121,2015

[16] K. Vijayakumar, A. J. Basanth, R. Karthikeyan, V.Sivakumar, N. Balamurugan, and C. S. Sundaram, "Influence of iron powder core on the switched reluctance motor performance enhancement," *Materials Today: Proceedings*, vol. 33, pp. 2255–2263, 2020, doi.org/10.1016/j.matpr.2020.04.082

[17] N. Arbab, W. Wang, C. Lin, J. Hearron, and B. Fahimi, "Thermal modeling and analysis of a double-stator switched reluctance motor," *IEEE Transactions on Energy Conversion.*, vol. 30, pp. 1209–1217, Sep 2015, doi: 10.1109/TEC.2015.2424400

[18] M. S. Rahman, G. F. Lukman, P. T. Hieu, K. I. Jeong, and J. W. Ahn, "Optimization and Characteristics Analysis of High Torque Density 12/8 Switched Reluctance Motor Using Metaheuristic Gray Wolf Optimization Algorithm," *Energies*, vol. 14, no. 7, p. 2013. Apr. 2021, doi.org/10.3390/en14072013.

[19] Y. Zhu, "*The Key Technologies for Powertrain System of Intelligent Vehicles Based on Switched Reluctance Motors,"* Springer. 2022. Doi.org/10.1007/978-981-16-4851-9.

[20] S. Allirani, H. Vidhya, T. Aishwarya, T. Kiruthika, and V. Kowsalya, "Design and performance analysis of switched reluctance motor using ANSYS Maxwell," in *2018 2nd International Conference on Trends in Electronics and Informatics (ICOEI)*, May. 2018, pp. 1427–1432. DOI: 10.1109/ICOEI.2018.8553912.

[21] B.Gecer, and N. F. O.,Serteller, "Understanding Switched Reluctance Motor Analysis using ANSYS/Maxwell," *IEEE International Symposium on Industrial Electronics*, Jun. 2020, pp. 446–449. doi: 10.1109/ISIE45063.2020.9152513.